X-ray Scattering Study of Hagfish Protease Inhibitor, a Protein Structurally Related to Complement and α_2-Macroglobulin†

Ragnar Österberg,* Bo Malmensten, and Atsushi Ikai‡

Department of Chemistry, Swedish University of Agricultural Sciences, S-750 07 Uppsala, Sweden

Received October 25, 1990; Revised Manuscript Received March 22, 1991

ABSTRACT: A protease inhibitor from hagfish blood plasma, homologous to human α_2-macroglobulin, has been studied in solution using small-angle X-ray scattering; the radius of gyration, R, was found to be 7.0 nm, the molecular weight 340 000 ± 20 000, and the largest distance within the molecule, D_{max}, 22 nm. When the inhibitor reacts with chymotrypsin, its 1:1 chymotrypsin complex is found to be more compact than the native molecule, R = 6.1 nm. A very similar conformational change is observed after the protein is reacted with methylamine. The data are consistent with models consisting of two equal elliptic cylinders with the same size as the one used as a model for the complement proteins C3 and C4 [cf. Österberg et al. (1989) *Eur. J. Biochem. 183*, 507–511]. In the model for the native protein, these cylinders are arranged in an extended form, and in the one for the methylamine derivative (or chymotrypsin complex), they are closer together so that the projection of their elliptic surfaces forms an angle of about 70°. These models for the hagfish protease inhibitor were expanded to models for the twice as large human α_2-macroglobulin using symmetry operations, and the resulting α_2-macroglobulin models were found to agree with those emerged from earlier studies involving electron microscopy and X-ray scattering methods.

The complement proteins C3 and C4 as well as α_2-macroglobulin are unique among mammalian proteins in the sense that they contain labile thiol ester bonds (Law et al., 1979; Tack et al., 1980; Janatova & Tack, 1981; Hostetter et al., 1982; Tack, 1983). When the complement proteins are activated via proteolytic cleavage of a peptide bond and when α_2-macroglobulin is subjected to proteolysis in the "bait" region, then their thioesters are cleaved. Thereby, via the activated glutamyl carboxylate group, the complement proteins may become covalently bound to the target particle and α_2-macroglobulin may bind and inactivate the proteases. Simultaneously, the proteins undergo dramatic conformational changes, where hidden surfaces of the proteins become exposed to the solvent (Isenmann et al., 1981; Isenmann & Kells, 1982; Nilsson & Nilsson, 1986; Delain et al., 1988; Österberg et al., 1988). As yet, the molecular backgrounds of these conformational changes are not thoroughly understood in terms of a general mechanism involving both the complement proteins and the 4 times larger macroglobulin molecule. Recently, we suggested that domain rotation may explain the conformational changes occurring within C3 (Österberg et al., 1989). Now, by studying the hagfish protease inhibitor, which is about twice as large as C3 and C4 and about half the size of α_2-macroglobulin (Osada et al., 1986), we extend the structural information obtained for C3 to include a protease inhibitor of the α_2-macroglobulin family of proteins. The shape of the hagfish protease inhibitor deduced from the present data and the mechanism suggested for "trapping" proteases by the inhibitor may be extended to α_2-macroglobulin, and the resulting models may explain the various pictures which have emerged from electron microscopy of human α_2-macroglobulin (Barrett et al., 1974; Schramm & Schramm, 1982; Nishigai et al., 1985; Tapon-Bretaudiere et al., 1985).

Materials and Methods

The protease inhibitor from hagfish was prepared from frozen hagfish blood plasma by using the method described by Osada et al. (1986). The purity of the final product was checked by polyacrylamide gel electrophoresis, giving just one single band before reduction and three bands after reduction of disulfide bonds [cf. Osada et al. (1986)].

Methylamine hydrochloride was obtained from Merck-Schuchardt (Munich, FRG). *N*-Ethylmaleimide (NEM) and phenylmethanesulfonyl fluoride (PMSF) were Sigma products. These compounds as well as all other chemicals used in this study were of analytical grade. Buffer A was 0.03 M Hepes, pH 7.5, containing 2 mM EDTA, 0.15 M NaCl, and 0.02% sodium azide.

The hagfish protease inhibitor was reacted with methylamine by first dialyzing it at 4 °C against buffer A of pH 8.0, containing 50 mM methylamine and 0.1 mM NEM, and then incubating it at 37 °C for 2 h. Complex formation between the protease inhibitor and chymotrypsin (Boehringer, Mannheim, Germany, catalog no. 103306) was studied in buffer A on solutions which had a molar ratio of inhibitor to enzyme of 1:1.2; it was incubated at 30 °C for 5 min, and then the resulting solution was dialyzed overnight against buffer A containing 30 μM PMSF and 0.1 mM NEM. The concentrations of the protease inhibitor and chymotrypsin were determined via the absorbance at 280 nm using $A^{1\%}_{1cm}$ = 7.8 and 15.0, respectively. In the case of the protease inhibitor, the absorbance factor was determined after analyses of C and N (Kirsten, 1971) and using the amino acid composition and carbohydrate content described previously (Osada et al., 1986).

Small-Angle X-ray Scattering. X-ray scattering data were collected with a Kratky camera (Kratky & Skala, 1958) in a room thermostated at 21 °C; data were measured up to a scattering angle, 2θ, of 0.12 rad. The primary data were transformed to absolute intensity data using a Lupolen sample (Kratky et al., 1966). After background substraction, the resulting data were deconvoluted with the slit width and slit length profiles of the primary beam and subjected to Fourier

† This work was supported by a grant from the Swedish Natural Science Research Council.

* Author to whom correspondence should be addressed.

‡ Present address: Laboratory of Biodynamics, Tokyo Institute of Technology, Yokohama, Japan.

0006-2960/91/0430-7873$02.50/0 © 1991 American Chemical Society

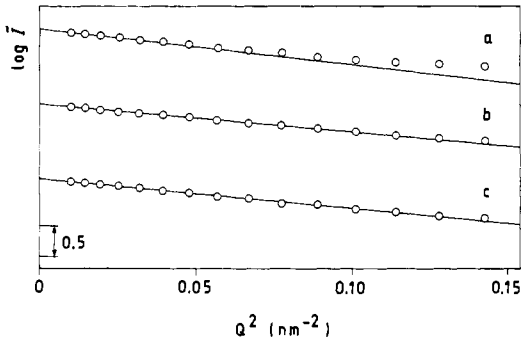

FIGURE 1: Guinier plots, log $\tilde{I}$ versus Q^2, for slit-smeared X-ray scattering data of hagfish protease inhibitor (a), its methylamine derivative (b), and its chymotrypsin complex (c). The statistical errors are less than a tenth of the circles representing the data. From the slopes of the straight lines, for $\tilde{R}Q \leq 1.3$, the radius of gyration for the slit-smeared data, $\tilde{R}$, was estimated. $Q = 4\pi(\sin\theta)/\lambda$, where 2θ is the scattering angle and λ the wavelength.

transformation using the computer program of Glatter (1977).

RESULTS

Figure 1 shows the proximal part of the absolute intensity X-ray scattering data recorded for the protease inhibitor both before and after reaction with methylamine in the form of Guinier plots. Also shown, in Figure 1, are the corresponding data obtained for solutions having a molar ratio of chymotrypsin to inhibitor of 1:1. The concentration dependence due to interparticular scattering was corrected for by extrapolating to $c = 0$, where c is the concentration in milligrams per milliliter; the range was 3–30 mg/mL.

After slit correction of the data (Glatter, 1974, 1977), the radius of gyration, R, was determined to be 7.0 ± 0.2 nm for the protease inhibitor and 6.2 ± 0.2 nm for its methylamine compound. These R values were evaluated by integration of the distance distribution function, $p(r)$ (Glatter, 1977), and, within the limits of experimental error, they agree with those obtained via the Guinier plots. Before slit correction, these values were 6.4 and 5.6 nm, respectively. The molecular mass was found to be essentially the same for the protease inhibitor both before and after reaction with methylamine: 340 000 ± 20 000. In these calculations, we used a partial specific volume, $v_2 = 0.707$ mL/g, which was determined by using a precise digital densitometer developed by Kratky et al. (1969). The molecular weight of the same protein determined previously by sedimentation equilibrium was reported to be 390 000 using an estimated partial specific volume of 0.73 mL/g (Osada et al., 1986). However, when the present v_2 value of 0.707 mL/g is used, this molecular weight, obtained via sedimentation equilibrium data, becomes 358 000; thus, the results of the two different methods agree within the limits of experimental errors.

The scattering data were further analyzed by calculating the distance distribution function, $p(r)$, using a computer program (Glatter, 1977); the result is shown in Figures 2 and 3. Although the value for the maximum distance within the particle (D_{max}) decreases from 21.5 to 19 nm when methylamine reacts with the inhibitor, these data are within the estimated experimental errors of ±2 nm. Nevertheless, it follows from Figures 2 and 3 that the very broad maximum in the $p(r)$ curve of the native protein becomes less broad in the corresponding curve obtained for the methylamine-reacted protein. Thus, the $p(r)$ curve as well as the change in the radius of gyration, $\Delta R = -0.8$ nm, indicates that the inhibitor molecule becomes more compact after the reaction with methylamine.

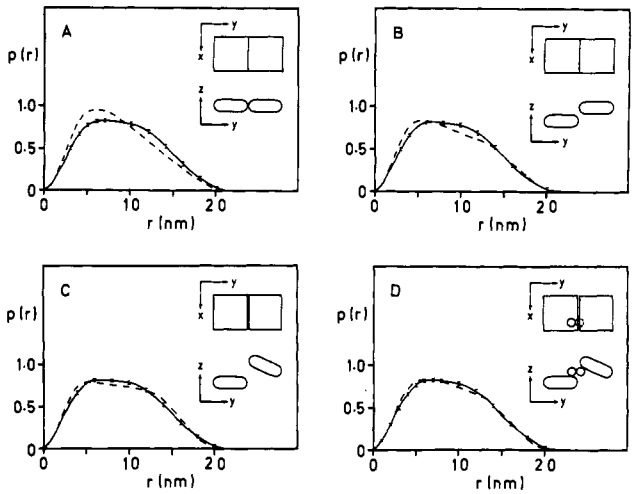

FIGURE 2: Distance distribution functions, $p(r)$, calculated from X-ray data recorded from the hagfish protease inhibitor, as indicated by solid curves with error bars, compared to those of models (dashed curves). For further explanations, see the text.

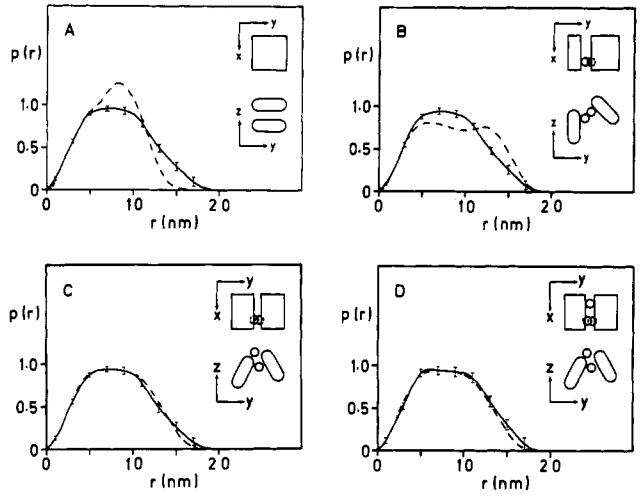

FIGURE 3: Distance distribution functions, $p(r)$, calculated from X-ray data recorded from the methylamine derivative of hagfish protease inhibitor (A–C) and for the chymotrypsin complex of this inhibitor (D), as indicated by solid curves with error bars, compared to those of models (dashed curves).

The data recorded from solutions of chymotrypsin and the protease inhibitor gave a somewhat higher molecular weight, 370 000 ± 20 000, in agreement with a 1:1 complex. The radius of gyration obtained, $R = 6.1$ nm, and the $p(r)$ curve obtained for the chymotrypsin complex are very similar to those of the methylamine derivative of the inhibitor (Figure 3). This indicates that the methylamine reaction quite closely simulates the inhibiting reaction of the protease, at least as far as the conformational change of the inhibitor is concerned.

Comparison with Models. In order to calculate the scattering from models and the corresponding distance distribution function, $p(r)$, we used a finite element method (small identical spheres) and the computer program developed by Glatter (1980). The radius of the spheres was 0.3 nm and the center to center distance 0.5 nm. The criteria used to decide whether or not the $p(r)$ curve of a model fitted the experimental one were the agreements obtained regarding the main peak(s), the D_{max} value, and the radius of gyration. A complete fit between the $p(r)$ curve of the multidomain inhibitor molecule [cf. Osada et al. (1986)] and that of an essentially compact model did not seem feasible, due to the contribution to the experimental curve from the electron density variation within the molecule.

However, these models were preferred where the $p(r)$ curves described the data as closely as possible within the error bars. Also, it should be kept in mind that, using a limited number of parameters, the present models are primarily designed to illustrate the methylamine and protease reactions of the inhibitor in schematic structural terms, rather than giving $p(r)$ curves that fit precisely to those of the experimental data.

At first, we used a model consisting of two prolate ellipsoids positioned parallel to each other (Osada et al., 1986); however, such a model yields two well-defined peaks or, if the ellipsoids are positioned quite close together, at least one fairly steep peak and a dominating shoulder. As shown by Figure 2, our experimental curve contains only one very broad maximum and virtually no shoulders or bumps. Then, as the next model, we used a model similar to the one described for half the human α_2-macroglobulin in an electron microscopic study (Delain et al., 1988); however, the $p(r)$ curve calculated from this model showed one steep maximum, and the error bars of the experimental curve were outside this calculated curve.

In the next step, we made use of the model which described the shape of the complement proteins C4 (Österberg et al., 1984) and C3 (Österberg et al., 1989). [Here, it should be noted that the projection of this model on the xy plane (cf. Figure 2) yields the dimensions 11 × 11 nm, which is in good agreement with a recent electron microscopic study (Ikai et al., 1990); however, most likely due to the flexibility of the molecule, the arms of the U- and V-shaped molecules, as shown in the electron micrographs (Ikai et al., 1990), may come together in solution so that the shapes of the molecules cannot be distinguished from that of a compact molecule (Österberg et al., 1989).] This model consists of an elliptic cylinder with the semiaxes 2.1 and 5.5 nm and a length of 11 nm. Since the hagfish protease inhibitor is about twice as large as C3 or C4, we combined two such cylinders into a model for the present inhibitor. Figure 2A shows the $p(r)$ curve obtained when the two elliptic cylinders are situated sideways, being connected along the 11-nm side. Here, the fit to the experimental data is much better than that of the two other models described above. However, some deviation remains (Figure 2A). It should be noted that this model can be almost precisely inscribed within the elliptic cylinder model (semiaxes 2.2 and 9.6 nm and length 11 nm) which gave the best fit to X-ray scattering data recorded from half the human α_2-macroglobulin (Sjöberg et al., 1985). Then, the positions of the two cylinders relative to each other were systematically varied regarding the distance from each other and the angles between their main axes in the xy and zy planes. For each position, a $p(r)$ curve was calculated; in all, about 25 different models were analyzed in this way (for an example, see Figure 2B). The calculated curves which gave the best fit to the experimental data are shown in Figure 2C,D. It should be noted that the model corresponding to the curve in Figure 2C has the two cylinders completely separated; the connecting protein structure is supposed to be quite small so that it does not contribute to the scattering intensity. In Figure 2D, two minor domains are tentatively introduced in order to connect the two cylinders; they are similar to the spherical domain suggested to be involved in the C3 structure (Österberg et al., 1989). It is worth noting that the models used for the calculation of the $p(r)$ curves in Figure 2A–D have projections on the xy plane that appear similar to certain electron microscopic pictures reported by Osada et al. [(1986); see, e.g., Figure 18b in their publication]; the differences may, to a certain extent, reflect the differences in shape observed from electron micrographs (favoring parts of the molecule with high electron density) and X-ray scattering (involving free movements of the particles in solution and spherical average at the data analysis).

When the protease inhibitor reacts with methylamine, the radius of gyration decreases (ΔR = −0.8 nm), and the very broad maximum of the $p(r)$ curve changes into a somewhat narrower peak (Figure 3). Furthermore, D_{max} tends to decrease from 21.5 to 19 nm. In order to simulate the experimental $p(r)$ curve of the methylamine derivative of the protease inhibitor, the two major bodies of the Figure 2D model were stepwise rotated, one clockwise and the other counterclockwise, and, after each step, a $p(r)$ curve was calculated and compared to the experimental one. The result, which gave the best fit, is shown in Figure 3C. As indicated in this figure, the two cylinders are positioned so that their two large flat surfaces tend to cover each other and so that the two bodies form an open angle of about 70°; the small globular domains are tentatively supposed to move so that one is situated within the angle and the other is situated outside [cf. Figures 10–12 in Osada et al. (1986)]. It should be noted, however, that the resolution of X-ray scattering is not sufficient to establish the precise location of the low-density material which connects the major domains. Various other models, such as the ones shown in Figure 3A,B, where the flat surfaces of the two elliptic cylinders are parallel (Figure 3A) or where the elliptic cylinders are further apart (Figure 3B), yield $p(r)$ curves which show larger deviations between the calculated and experimental data. Finally, as shown in Figure 3D, a similar position of the two elliptic cylinders as that of the model displayed in Figure 3C also explains the data obtained for the chymotrypsin complex of the protease inhibitor. Here, a small body (with a volume corresponding to chymotrypsin) is tentatively introduced within the angle between the two flat surfaces of the elliptic cylinders.

In conclusion, the hagfish protease inhibitor, the molecular mass of which is about twice as large as those of the complement proteins C3 and C4, can readily be explained by using a model (Figure 2D) which consists of two copies of the one previously used to describe the shape of C3 (Österberg et al., 1989) and C4 (Österberg et al., 1984). By changing the position of these two models relative to each other, we obtain models from which calculated scattering data yield good agreement with the experimental data recorded from the methylamine derivate as well as the chymotrypsin complex of the inhibitor (Figure 3C,D).

Discussion

The results presented in the previous section indicate that monomeric, dimeric, and tetrameric thiol ester proteins are structurally related. The elliptic cylinder model which explains the shapes of C3 and C4 (Österberg et al., 1989, 1984) is also found to explain the X-ray scattering from the hagfish protease inhibitor. As shown by Figure 2D, two of the C3 shape models, positioned in a fairly extended form and connected via two minor globular domains, essentially explain the experimental $p(r)$ curve within the limits of experimental errors. Likewise, a shape model for half-molecules of human α_2-macroglobulin (Sjöberg et al., 1985) can almost precisely circumscribe two C3 shape models of elliptic cylinders, when they are connected sideways (Figure 2A). Furthermore, similar kinds of elliptic cylinders, but not identical with the present ones, were previously used in order to explain the shape of human α_2-macroglobulin (Österberg & Malmensten, 1984).

This similarity in shape among the thiol ester proteins supports the idea that they may be genetically related [see, e.g., Starkey (1983)]. In an evolutionary study on vertebrate

and invertebrate α_2-macroglobulin homologues (Starkey & Barrett, 1982a), a dimeric homologue with a molecular weight of 360 000 was prepared from plaice (Starkey et al., 1982). It was suggested that α_2-macroglobulin first appeared as a protein of 360 kDa in an ancestor of all modern vertebrates (Starkey & Barrett, 1982b). More recently, dimeric homologues have also been prepared from other sources, such as hagfish (Osada et al., 1986), southern grass frog (Feldman & Pizzo, 1986), lobster (Spycher et al., 1987), horseshoe crab (Armstrong & Quigley, 1987), and crayfish (Hergenhahn et al., 1988). The evolutionary relationship between these dimeric thioester proteins and the tetrameric human α_2-macroglobulin is further indicated by similarities in the primary structure (Hall et al., 1989; Sottrup-Jensen et al., 1990). The crayfish and horseshoe crab proteins showed homology in amino acid sequences, not only with human α_2-macroglobulin but also with the complement proteins C3 and C4. It was concluded that these sequences must have been conserved during more than 550 million years of evolutionary divergence of the arthropodial and vertebrate lineages (Sottrup-Jensen et al., 1990).

When human α_2-macroglobulin reacts with methylamine, it undergoes a marked conformational change (Barrett et al., 1979). As indicated by the X-ray scattering method, the molecule becomes more compact; the radius of gyration, R, decreases from 7.8 to 7.2 nm, and there is a change in the side maximum (Österberg & Malmensten, 1984). [Boisset et al. (1989) recently reported the same R value for the native α_2-macroglobulin, but they observed a ΔR value of -1.0 ± 0.4 nm.] Trypsin reaction followed by binding of two trypsin molecules per molecule of α_2-macroglobulin (Branegård et al., 1982) yields a result similar to, but not identical with, that of the methylamine derivative (Österberg & Malmensten, 1984; Boisset et al., 1989). In the present study, the methylamine reaction of the hagfish protease inhibitor appears to give a similar decrease in the R value with $\Delta R = -0.8$ nm. Also, as indicated by Figure 3C, the $p(r)$ curve of the methylamine derivative can be explained by the scattering from a model where the two elliptic cylinders are rearranged into a more compact model. Furthermore, the conformational change obtained after the reaction with chymotrypsin (Figure 3D) appears to be virtually identical with that observed for the methylamine derivative (Figure 3C).

The methylamine sensitivity of the hagfish inhibitor [cf. Osada et al. (1986)] appears to be similar to, but not identical with, that of the other dimeric proteins studied so far. Thus, after the reaction with methylamine, the ability of all these proteins to inhibit proteinases seems to be abolished. However, for the plaice protein, neither the reaction with the methylamine nor the reaction with a proteinase gave any change in the electrophoretic movement relative to that of the native protein ("slow to fast" conformational change) (Starkey et al., 1982). The lobster protein, on the other hand, showed a "slow to fast" conformational change after reaction with a proteinase but not after reaction with methylamine (Spycher et al., 1987). This behavior is quite different from that found in bovine α_2-macroglobulin, which does not show the "slow to fast" conformational change after reaction with methylamine but remains at least partly active (Björk et al., 1985). The same is true for ovomacroglobulin (Nagase et al., 1983), but in this case, it may be due to a lack of thiol ester bonds (Nagase & Harris, 1983). Although one idea is that the conformational change is triggered by the thiol ester bond cleavage, it seems to be kinetically retarded in varying degree by an uncleaved peptide chain, and quite different kinetics are observed for the methylamine-induced conformational change among the thioester proteins [for a discussion on this subject, see Spycher et al. (1987)]. Also, thiol ester bond cleavage is not the ultimate requirement for the conformational change, since it also occurs in ovomacroglobulin.

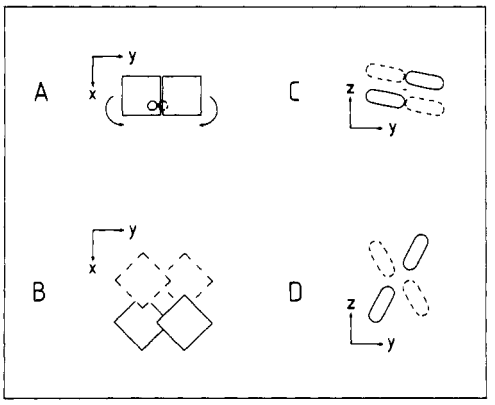

FIGURE 4: Schematic reconstruction of models for human α_2-macroglobulin using the models for the hagfish protein from Figures 2D and 3C. The domains corresponding to parts B–D are supposed to be connected via low electron density regions not shown in the figures. (A) Projection of the Figure 2D model on the xy plane. Flexibility of the inhibitor is supposed to allow rotations of the two major domains around axes parallel to the z axis. (B) Projection of the Figure 2D model on the xy plane after rotation of the two major bodies (solid lines), [cf. Osada et al. (1986)]. The addition of a second copy of this model (dashed lines) yields an α_2-macroglobulin model [cf. Figure 3A in Nishigai et al. (1985), Figure 1c in Tapon-Bretaudiere et al. (1985), and Figure 1A in Ikai et al. (1987)]. (C) Projection of the major bodies of the Figure 2D model on the zy plane after slight rotation so that they become related via the 2-fold axis indicated (solid lines). The addition of a second copy (dashed lines) with the same symmetry yields an α_2-macroglobulin model of the H-type (Österberg & Malmensten, 1984) (see the text). (D) Projection of the major bodies of the Figure 3C model on the zy plane (indicated by solid and dashed lines). The addition of a second copy (dashed and solid lines) related to the first one via a 2-fold axis parallel with the x axis yields an α_2-macroglobulin model looking like the outer lines of the Cyrillic letter (English transliteration zh). As indicated by dashed and solid lines, the projection displayed can also be obtained via the Figure 4C model (see the text).

In order to gain a detailed understanding of the molecular mechanism involved, when the α_2-macroglobulin proteins bind and inhibit proteinases and undergo a major conformational change, information about the three-dimensional structure would be necessary. A first step in this direction is a series of electron microscopic studies. However, the pictures emerging from these studies are somewhat puzzling: some of the early pictures showed structures looking like a Cyrillic letter (English transliteration zh) (Barrett et al., 1974; Schramm & Schramm, 1982), but the more recent pictures shows the four subunits exposed in a cloverleaf or a doughnut type of structure (Ikai et al., 1983; Tapon-Bretaudiere et al., 1985; Nishigai et al., 1985). We believe that the present results, which give both the shape of the hagfish protease inhibitor in the native form and the shape obtained after reaction with methylamine, may be used to illustrate the relationship between the structure of the hagfish protease inhibitor and that of human α_2-macroglobulin.

Our model for the native hagfish protease inhibitor (Figure 2D) may be used to illustrate a projection of the tetrameric homologue exposing its four subunits, for instance, in a doughnut configuration. Figure 4A shows a projection of the present Figure 2D model when we look down the z axis (using the same axis system as those of Figures 2 and 3). We assume that there might be some flexibility within the connecting globular domains and rotations around axes parallel to the z axis, as indicated in Figure 4A, may lead to a model like the

fully drawn picture in Figure 4B. Such a rotation might be related to "hinge bending and folding" and may not necessarily lead to a change in conformational energy within the molecule [Huber & Bennett, 1987; Faber & Matthews, 1990; cf. Dobson (1990)]. Then we form a tetramer by introducing a second model of the same kind (dashed lines) by generating it via a 2-fold axis parallel to the z axis. As shown by Figure 4B, the projection of the resulting model looks very similar to the doughnut configuration in electron microscopy of the α_2-macroglobulin (Nishigai et al., 1985; Tapon-Bretaudiere et al., 1985; Ikai et al., 1987). Such a conformation might be favored due to some restriction in the free movements of the molecule imposed by the electron microscopy conditions. On the other hand, a projection on the zy plane may lead to an H-like model (Figure 4C). Here, we first slightly rotate the two elliptic cylinders of Figure 2D (or Figure 2C) so that they become related via a 2-fold axis. [Although such a model yields a $p(r)$ curve, which does not fit the experimental one as well as that of Figure 2D, it is one of a number of possible models.] Then, a second copy with the same symmetry is introduced, forming a tetramer (Figure 4C). For clarity, the tentative models of the minor globules, mainly based on electron microscopic data, are excluded in Figure 4 [cf. Boisset et al. (1989)]. One may imagine that this extended H-like conformation might prevail in dilute solution, where the protein is allowed to move freely (Österberg & Malmensten, 1984). The difference between the conformations illustrated in Figure 4B,C may not necessarily be larger than the two extremes of conformation for the IgG molecule, where the Y form may correspond to Figure 4B and the extended "rod-like" form may correspond to Figure 4C (Huber & Bennett, 1987).

In agreement with the discussion above, the general idea is that native α_2-macroglobulin is a flexible molecule that may, to a certain extent, vary its shape due to the restrictions caused by the environment (Tapon-Bretaudiere et al., 1985; Delain et al., 1988). When human α_2-macroglobulin reacts with methylamine or when it reacts with proteinases, the resulting conformational change is supposed to stabilize the structure and decrease the flexibility. As shown by Figure 3, reactions of the inhibitor with either methylamine or chymotrypsin give essentially the same $p(r)$ curve. The data can be explained by a model where the two elliptic cylinders, to a certain extent, cover each other and form an angle of about 70°. Now, if we add a second copy of the model projected on the zy plane in Figure 3C, so that the second copy is related to the first one via a 2-fold axis parallel with the x axis, then we obtain a model, the zy projection of which will resemble the Cyrillic letter (English transliteration zh); the projections of the major bodies involved are shown in Figure 4D. However, as indicated by dashed and solid lines in Figure 4D, this particular model can also, in principle, be obtained from Figure 4C by moving the major bodies of each "dimer" in opposite directions. When going from the hagfish dimer to human α_2-macroglobulin, this folding process would then only be possible if we assume that, once tetrameric α_2-macroglobulin was formed, mutations had taken place [cf. Starkey (1983)] that allowed "folding" of the molecule as illustrated by Figure 4C,D. It is then tempting to speculate that these latter movements of the major domains, as illustrated by going from Figure 4C to Figure 4D, may also correspond to the formation of the "trap" (Barrett & Starkey, 1973), when two proteinases are bound and inhibited by α_2-macroglobulin.

Acknowledgments

We express our sincere gratitude to the Marine Biological Laboratory of the University of Tokyo for collection of the hagfish used in this study and to Drs. H. Arakawa and T. Boive for technical assistance.

Registry No. C3, 80295-41-6; C4, 80295-48-3; proteinase inhibitor, 37205-61-1.

References

Armstrong, P. B., & Quigley, J. P. (1987) *Biochem. J. 248*, 703–707.

Barrett, A. J., & Starkey, P. M. (1973) *Biochem. J. 133*, 709–724.

Barrett, A. J., Starkey, P. M., & Munn, E. A. (1974) in *Proteinase Inhibitors*, (Fritz, H., Tshesche, H., Green, L. J., & Truscheit, E., Eds.) pp 72–77, Springer-Verlag, Berlin.

Barrett, A. J., Brown, M. A., & Sayers, C. A. (1979) *Biochem. J. 181*, 401–418.

Björk, I., Lindblom, T., & Lindahl, P. (1985) *Biochemistry 24*, 2653–2660.

Boisset, N., Taveau, J.-C., Pochon, F., Tardieu, A., Barray, M., Lamy, J. N., & Delain, E. (1989) *J. Biol. Chem. 264*, 12046–12052.

Branegård, B., Österberg, R. & Sjöberg, B. (1982) *Eur. J. Biochem. 122*, 663–666.

Delain, E., Barray, M., Tapon-Bretaudiere, J., Pochon, F., Marynen, P., Cassiman, J.-J., Van den Berghe, H., & Van Leuven, F. (1988) *J. Biol. Chem. 263*, 2981–2989.

Dobson, C. M. (1990) *Nature 348*, 198–199.

Faber, H. R., & Matthews, B. W. (1990) *Nature 348*, 263–266.

Feldman, S. R., & Pizzo, S. V. (1986) *Biochemistry 25*, 721–727.

Glatter, O. (1974) *J. Appl. Crystallogr. 7*, 147–153.

Glatter, O. (1977) *J. Appl. Crystallogr. 10*, 415–421.

Glatter, O. (1980) *Acta Phys. Austriaca 25*, 243–256.

Hall, M., Söderhäll, K., & Sottrup-Jensen, L. (1989) *FEBS Lett. 254*, 111–114.

Hergenhahn, H. G., Hall, H., & Söderhäll, K. (1988) *Biochem. J. 255*, 801–806.

Hostetter, M. K., Thomas, M. L., Rosne, F. S., & Tack, B. F. (1982) *Nature 282*, 72–75.

Huber, R., & Bennett, W. S. (1987) *Nature 326*, 334–335.

Ikai, A., Kitamoto, T., & Nishigai, M. (1983) *J. Biochem. 93*, 121–127.

Ikai, A., Nishigai, M., Osada, T., Arakawa, H., & Kikuchi, M. (1987) *J. Protein Chem. 6*, 81–93.

Ikai, A., Nishigai, M., Saito, A., Sinohara, H., Muto, Y., & Arata, Y. (1990) *FEBS Lett. 260*, 291–293.

Isenmann, D. E., Kells, D. I. C., Cooper, N. R., Müller-Eberhard, H. J., & Pangburn, M. K. (1981) *Biochemistry 20*, 4458–4467.

Isenmann, D. E., & Kells, D. I. C. (1982) *Biochemistry 21*, 1108–1117.

Janatova, J., & Tack, B. F. (1981) *Biochemistry 20*, 2394–2402.

Kirsten, W. (1971) *Microchem. J. 16*, 610–625.

Kratky, O., & Skala, Z. (1958) *Z. Electrochem. 62*, 73–77.

Kratky, O., Pilz, I., & Schmitz, P. J. (1966) *J. Colloid Sci. 21*, 24–34.

Kratky, O., Leopold, H., & Stabinger, H. (1969) *Z. Angew. Phys. 27*, 273–275.

Law, S. K., Lichtenberg, N. A., & Levine, R. P. (1979) *J. Immunol. 123*, 1388–1394.

Nagase, H., Harris, E. D., Jr., Woessner, J. F., Jr., & Brew, K. (1983) *J. Biol. Chem. 258*, 7481–7489.

Nagase, H., & Harris, E. D., Jr. (1983) *J. Biol. Chem. 258*, 7490–7498.

Nishigai, M., Osada, T., & Ikai, A. (1985) *Biochim. Biophys. Acta 831*, 236–241.

Nilsson, U., & Nilsson, B. (1986) *Scand. J. Immunol. 23*, 357–363.

Osada, T., Nishigai, M., & Ikai, A. (1986) *J. Ultrastruct. Mol. Struct. Res. 96*, 136–145.

Österberg, R., Eggertsen, G., Lundwall, Å., & Sjöquist, J. (1984) *Int. J. Biol. Macromol. 6*, 195–198.

Österberg, R., & Malmensten, B. (1984) *Eur. J. Biochem. 143*, 541–544.

Österberg, R., Malmensten, B., Nilsson, U., Eggertsen, G., & Kjems, J. (1988) *Int. J. Biol. Macromol. 10*, 15–20.

Österberg, R. Nilsson, U., Stigbrand, T., & Kjems, J. (1989) *Eur. J. Biochem. 183*, 507–511.

Schramm, H. J., & Schramm, W. (1982) *Hoppe-Seyler's Z. Physiol. Chem. 363*, 803–812.

Sjöberg, B., Pap, S., & Kjems, J. (1985) *Eur. Biophys. J. 13*, 25–30.

Sottrup-Jensen, L., Borth, W., Hall, M., Quigley, J. P., & Armstrong, P. B. (1990) *Comp. Biochem. Physiol. 96B*, 621–625.

Spycher, S. E., Araya, S., Isenmann, D. E., & Painter, R. H. (1987) *J. Biol. Chem. 262*, 14606–14611.

Starkey, P. M. (1983) *Ann. N.Y. Acad. Sci. 421*, 112–118.

Starkey, P. M., & Barrett, A. J. (1982a) *Biochem. J. 205*, 91–95.

Starkey, P. M., & Barrett, A. J. (1982b) *Biochem. J. 205*, 105–115.

Starkey, P. M., Fletcher, T. C., & Barrett, A. J. (1982) *Biochem. J. 205*, 97–104.

Tack, B. F. (1983) *Springer Semin. Immunopathol. 6*, 259–289.

Tack, B. F., Harrison, R. A., Janatova, J., Thomas, M. L., & Prahl, J. W. (1980) *Proc. Natl. Acad. Sci. U.S.A. 77*, 5766–5768.

Tapon-Bretaudiere, J., Bros, A., Couture-Tosi, E., & Delain, E. (1985) *EMBO J. 4*, 85–89.